Offprints from
Water and Aqueous Solutions
Edited by R. A. Horne
Published by John Wiley & Sons, Inc., 1972

8 Aspects of the Statistical-Mechanical Theory of Water

A. Ben-Naim and F. H. Stillinger, Jr.,
Bell Telephone Laboratories, Incorporated,
Murray Hill, New Jersey

Abstract

The prospects are examined for construction of a fundamental and systematic theory of liquid water, utilizing the techniques of classical statistical mechanics for rigid asymmetric rotors. For that purpose, a tentative molecular pair potential is proposed which exhibits the known tendency toward tetrahedral coordination and which fits the measured water-vapor second virial coefficient reasonably well. Several potential curves are displayed for the more important classes of pair configurations. By means of indirect calculations, we have established a local cooperative tendency for orientational correlation of neighboring water molecules in arrangements suitable for hydrogen bonding. Finally, we stress the relevance and importance of Monte Carlo calculations (with electronic computers) designed literally to provide submicroscopic pictures of the random hydrogen-bond networks in liquid water and aqueous solutions.

1 Introduction

The study of liquid water could superficially be considered as a single branch of the entire field of liquid-state research. However, it is obvious that this one substance occupies a place of special prominence, not only because of its unique physical characteristics but also because it seems to be the only fluid medium capable of supporting biochemical processes. No doubt these peculiar properties arise from the same molecular feature that has thus far prevented development of a serious first-principles theory of liquid water, namely, the noncentral forces operative between the molecules.

The earliest attempts to understand the behavior of water apparently stemmed from Röntgen's[1] suggestion that the liquid contained "ice molecules." Chadwell[2] has reviewed a number of these phenomenological treatments of water in terms of association complexes. Since little was known

about molecular structure and intermolecular forces during the early period, however, these treatments were necessarily very limited in scope.

In 1933, Bernal and Fowler[3] provided a major conceptual advance by pointing out the propensity for water molecules to bond to one another with locally tetrahedral geometry. In varying degrees, this structural feature has seemed to affect, if not to dominate, all subsequent attempts to explain the properties of liquid water (and aqueous solutions) in a statistical-mechanical context.[4] Even so, mere emphasis on tetrahedral coordination amounts to far less than complete mechanical description of the nature of water-molecule interactions.

The modern trend in formal liquid-state theory seeks to establish a clear quantitative connection between carefully specified intermolecular potentials (as the starting point) and various molecular distribution functions and thermodynamic properties implied by those potentials.[5] Satisfying success has been achieved in this approach for simple substances such as argon, not only because the relevant central pair potentials are rather well established but also because reliable integral equation methods are available for computation of the requisite radial distribution functions.

In this chapter we attempt to lay the groundwork for a corresponding formal statistical-mechanical theory of liquid water. For that purpose we presume (at least initially) that the total potential energy is composed of a pairwise-additive sum of pair potentials. Even in the case of argon this is not rigorously true, but it is reasonable to regard three-body forces, and so on, as mild perturbations on the pairwise-additivity model that may be accounted for at the end of the primary calculation. The next section is devoted to certain immediate implications of the pair-potential assumption, and we record there the corresponding exact formal expressions for the mean energy, the pressure, the compressibility, and some further quantities requiring at most knowledge of the water pair-distribution function.

Section 3 exhibits what we consider to be analytically one of the simplest water-molecule pair potentials that still retains certain essential features of the actual situation. It represents a modification and extension of Bjerrum's four-point-charge electrostatic model of the water molecule,[6] and inherently favors tetrahedral coordination.

The second and third virial coefficients for water vapor are examined in Section 4. By demanding that the theoretical expression for the first of these (with our suggested potential function) agree with experiment, certain free parameters in the potential are determined.

Section 5 is devoted to preliminary theoretical investigation of the pair-correlation function for liquid water. Whereas for substances such as argon with central molecular forces, this quantity (at fixed temperature and pressure) depends only on scalar distance, the full pair-correlation function for

water is vastly more complicated. In order to fix the relative configuration and orientation of two water molecules, a minimum of *six* variables must be specified. With this formidable feature in mind, we assess the practical utility of the Percus–Yevick integral equation for the water pair-correlation function. In addition, we examine in Section 5 a semiempirically determined pair-correlation function in order to estimate the cooperative character of orientational ordering in liquid water.

The final discussion, Section 6, attempts to predict the most useful course of future research directed to the construction of a full fundamental statistical mechanical theory of liquid water.

2 Pair-Potential Assumption

The free water molecule is a nonlinear triatomic species exhibiting C_{2v} symmetry. The average bond angle is about 105°, only slightly less than the geometrically ideal angle

$$\theta_T = 109°28' \tag{1}$$

between lines connecting the center of a regular tetrahedron to its vertices. The oxygen–hydrogen bond lengths in the isolated molecule are 0.96 Å, but in condensed phases such as ice and liquid water these lengthen perhaps to 1.00 Å on the average.[7]

In order to describe the position and orientation of a water molecule in space, six variables are required. We shall take these to be, first, the vector position $\mathbf{r} = (x, y, z)$ of the oxygen nucleus, and second, the set of Euler angles ϕ, θ, ψ required to fix the orientation of the molecule, regarded as a rigid body. Figure 1 and Figures 2*a* to *c* establish the particular Euler angle convention that we have employed.

Our primary intention is to describe liquid water by the techniques of classical statistical mechanics. The central quantity in that discipline is the canonical partition function, Q_N. Since we regard the individual water molecules as acting toward one another as rigid asymmetric rotors, the partition function has the following form:

$$Q_N = \frac{1}{N!}\left[\frac{(2\pi kT)^3 m^{3/2}(I_1 I_2 I_3)^{1/2}\, Q_{\text{vib}}}{h^6}\right]^N \times \int d\mathbf{x}_1 \cdots \int d\mathbf{x}_N \exp\left[-\beta V_N(\mathbf{x}_1 \cdots \mathbf{x}_N)\right], \qquad \beta = (kT)^{-1} \tag{2}$$

In this expression, m is the molecular mass, the I's are the three moments of inertia, Q_{vib} is the partition function for the vibrational degrees of freedom

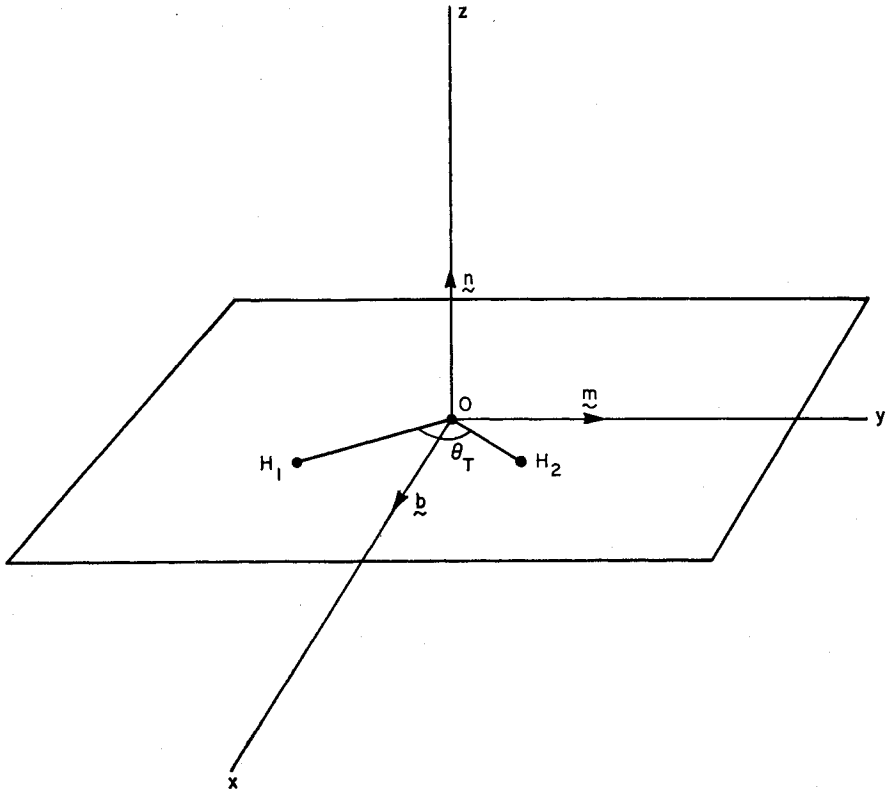

Figure 1. Coordinate axes for the rigid nonlinear water molecule. Cartesian axes x, y, z are fixed; orthogonal unit vectors **b**, **m**, **n** rotate with the molecule. **b** is the molecule's symmetry axis, **m** is in the molecular plane, and $\mathbf{n} = \mathbf{b} \times \mathbf{m}$.

of an isolated water molecule, and V_N is the total potential of interaction between the N molecules in the system.

Vector $\mathbf{x}_j$ in (2) stands for the six coordinates specifying position and orientation of molecule j, and the $\mathbf{x}$ integrations in more detail must be carried out as follows:

$$\int d\mathbf{x}_j \equiv \int_V d\mathbf{r}_j \int_0^{2\pi} d\phi_j \int_0^{\pi} \sin\theta_j \, d\theta_j \int_0^{2\pi} d\psi_j \tag{3}$$

where V is the vessel volume containing the N water molecules.

Molecular distribution functions $\rho^{(n)}(\mathbf{x}_1 \cdots \mathbf{x}_n)$ give the probabilities that a set of differential volume-and-orientation elements $d\mathbf{r}_j \, d\phi_j \, d\theta_j \, d\psi_j$ $(j = 1 \cdots n)$

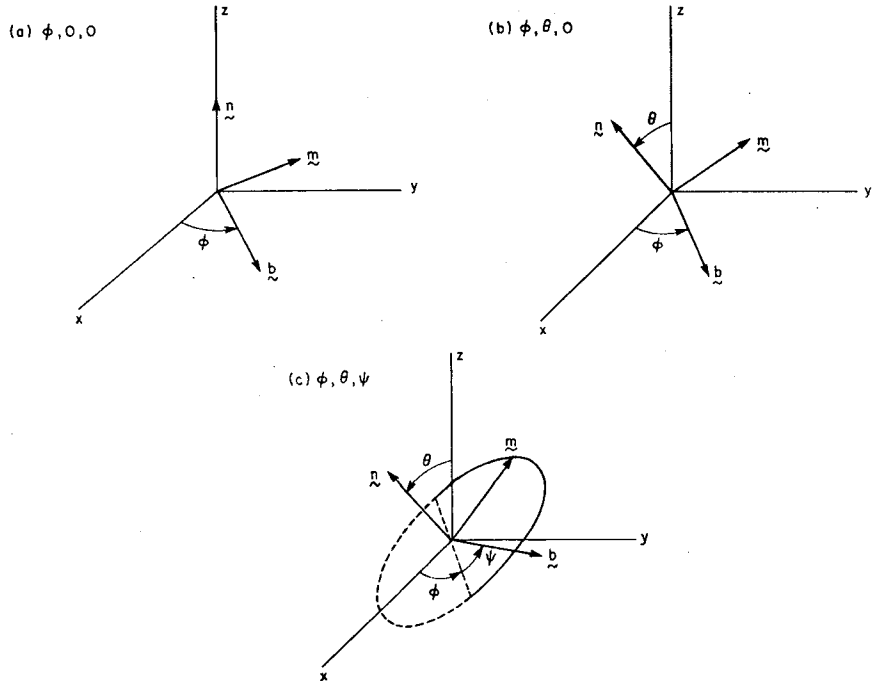

Figure 2. Euler angle convention for the water molecule. All three angles are 0 in the configuration shown in Figure 1. (*a*) φ increases from 0 by rotation about the initial **n** axis. (*b*) Rotation about the *new* **b** axis defines θ. (*c*) The last Euler angle, ψ, describes rotation about the *new* **n** direction. To generate all orientations uniquely, the limits $0 \leq \varphi, \psi \leq 2\pi$, and $0 \leq \theta \leq \pi$ must be imposed.

are simultaneously occupied by any of the water molecules. The precise definitions of the $\rho^{(n)}$ involve multiple integrals of the full configuration space canonical density

$$(4) \qquad \rho^{(n)}(\mathbf{x}_1 \cdots \mathbf{x}_n) = \frac{N! \int d\mathbf{x}_{n+1} \cdots \int d\mathbf{x}_N \exp\left[-\beta V_N(\mathbf{x}_1 \cdots \mathbf{x}_N)\right]}{(N-n)! \int d\mathbf{x}_1 \cdots \int d\mathbf{x}_N \exp\left[-\beta V_N(\mathbf{x}_1 \cdots \mathbf{x}_N)\right]}$$

Although this set of functions specifies the full orientation dependence for sets of n molecules, it suffices for some purposes merely to know the orientationally averaged densities; for that reason we also define the "contracted" molecular distribution functions

$$(5) \qquad \tilde{\rho}^{(n)}(\mathbf{r}_1 \cdots \mathbf{r}_n) = \int \sin\theta_1 \, d\phi_1 \, d\theta_1 \, d\psi_1 \cdots \int \sin\theta_n \, d\phi_n \, d\theta_n \, d\psi_n \, \rho^{(n)}(\mathbf{x}_1 \cdots \mathbf{x}_n)$$

Finally, correlation functions $g^{(n)}$ and $\bar{g}^{(n)}$ are introduced thus

$$\rho^{(n)}(\mathbf{x}_1 \cdots \mathbf{x}_n) = \left(\frac{N}{8\pi^2 V}\right)^n g^{(n)}(\mathbf{x}_1 \cdots \mathbf{x}_n)$$
$$\bar{\rho}^{(n)}(\mathbf{r}_1 \cdots \mathbf{r}_n) = \left(\frac{N}{V}\right)^n \bar{g}^{(n)}(\mathbf{r}_1 \cdots \mathbf{r}_n) \tag{6}$$

with the properties (in the infinitely large system limit) of approaching unity for wide separation of all positions $\mathbf{r}_1 \cdots \mathbf{r}_n$.

The potential energy, V_N, viewed from the most fundamental standpoint, is an enormously complicated function. Of course it comprises permanent dipole–dipole and dispersion interactions between molecules at moderate range, as well as hydrogen bonding at close range. But also it contains subtle many-body potentials, one aspect of which is the dielectric modification of dipole-dipole forces. In view of the separation of Q_{vib} (defined for *isolated* molecules) in (2) we must furthermore be prepared to admit that V_N will contain contributions from coupling of vibrations between neighboring molecules in the liquid phase.

In spite of these complications, there ought still to be a "best" choice of pair potential $v(\mathbf{x}_i, \mathbf{x}_j)$ such that the assumption

$$V_N(\mathbf{x}_1 \cdots \mathbf{x}_N) \simeq \sum_{i<j=1}^{N} v(\mathbf{x}_i, \mathbf{x}_j) \tag{7}$$

retains most essential features of the liquid-water problem. A reasonable sort of criterion for choice of v would be minimization of the squared deviation between Boltzmann factors for V_N and its pairwise-additive approximation by (7)

$$\int d\mathbf{x}_1 \cdots \int d\mathbf{x}_N \left\{ \exp\left[-\frac{\beta}{2} V_N(1 \cdots N)\right] - \exp\left[-\frac{\beta}{2} \sum_{i<j=1}^{N} v(i,j)\right] \right\}^2 = \text{minimum} \tag{8}$$

By setting the first variation with respect to v of this last expression equal to 0, we obtain the condition

$$\int d\mathbf{x}_3 \cdots \int d\mathbf{x}_N \exp\left\{-\beta\left[\tfrac{1}{2} V_N(1 \cdots N) + \tfrac{1}{2} \sum_{i<j=1}^{N} v(i,j)\right]\right\} = \int d\mathbf{x}_3 \cdots \int d\mathbf{x}_N \exp\left[-\beta \sum_{i<j=1}^{N} v(i,j)\right] \tag{9}$$

which must be obeyed for *all* $\mathbf{x}_1$ and $\mathbf{x}_2$. If we first take $\mathbf{r}_1$ and $\mathbf{r}_2$ to be far

apart in (9), we see that the canonical partition functions (and hence the Helmholtz free energies) for the two potential functions

$$\tfrac{1}{2}V_N + \tfrac{1}{2}\sum_{i<j=1}^{N} v(i,j) \tag{10}$$

and

$$\sum_{i<j=1}^{N} v(i,j) \tag{11}$$

must be identical. Furthermore, by taking $\mathbf{r}_1$ and $\mathbf{r}_2$ close to one another in (9), we also conclude that interactions (10) and (11) will produce identically the same pair distribution function $\rho^{(2)}(\mathbf{x}_1, \mathbf{x}_2)$.

Although we cannot conclude that the optimal pairwise-additivity approximation (7) causes *no* change in free energy or in the various $\rho^{(n)}$ for water, the invariances just mentioned in passing from (11) to (10), or "halfway" from pairwise additivity to the true V_N, indicate that (7) is generally an excellent approximation.

Variational principle (8) is unfortunately not suited for direct construction of a liquid-phase v. Furthermore, the pair potentials it requires might exhibit small temperature and density dependence. We take the point of view in the following paragraphs that a fixed $v(\mathbf{x}_i, \mathbf{x}_j)$ can be determined for liquid water by alternative means and that residual temperature and density dependence is negligible if we restrict attention to the behavior of liquid water at (or near) room temperature and 1 atm pressure.

The primary practical advantage of pairwise-additive potentials is that most of the usual thermodynamic properties can be expressed in terms of just v and $\rho^{(2)}$. The most straightforward of these is the mean energy per molecule

$$\begin{aligned}\frac{E}{N} &= \frac{E^{(0)}}{N} + \frac{1}{2N}\int d\mathbf{x}_1 \int d\mathbf{x}_2 v(\mathbf{x}_1, \mathbf{x}_2)\rho^{(2)}(\mathbf{x}_1, \mathbf{x}_2) \\ &= \frac{E^{(0)}}{N} + \frac{N}{16\pi^2 V}\int d\mathbf{x}_2 v(\mathbf{x}_1, \mathbf{x}_2) g^{(2)}(\mathbf{x}_1, \mathbf{x}_2)\end{aligned} \tag{12}$$

where $E^{(0)}/N$ is the mean molecular energy at the ambient temperature for the infinitely dilute vapor. The integral term in (12) merely counts molecular pairs in all possible pair configurations and accumulates the corresponding potential energy contributions.

The expression for the pressure, p, in virial form may be derived by a trivial generalization of Green's volume-scaling procedure for spherically symmetric molecules.[8] One obtains

$$\frac{pV}{NkT} = 1 - \frac{1}{6NkT}\int d\mathbf{x}_1 \int d\mathbf{x}_2 [\mathbf{r}_{12}\cdot\nabla_{\mathbf{r}_{12}} v(\mathbf{x}_1, \mathbf{x}_2)]\rho^{(2)}(\mathbf{x}_1, \mathbf{x}_2) \tag{13}$$

$$\mathbf{r}_{12} = \mathbf{r}_2 - \mathbf{r}_1$$

The isothermal compressibility

$$\kappa_T = -\frac{1}{V}\left(\frac{\partial V}{\partial p}\right)_T \tag{14}$$

has the unique advantage of being exactly expressible in terms of the pair-distribution function, quite irrespective of the pairwise-additivity assumption (7). Furthermore, only the angle-integrated quantity $\bar{\rho}^{(2)}$ is required. Provided that we first understand the infinite-system-size limit to have been taken for $\bar{\rho}^{(2)}$, the general compressibility relation is

$$kT\kappa_T = \frac{V}{N} + \int d\mathbf{r}_{12}[\bar{g}^{(2)}(\mathbf{r}_{12}) - 1] \tag{15}$$

The chemical potential, μ, may in principle be obtained via the Gibbs–Duhem relation

$$dp = \rho\, d\mu$$

at constant temperature, by integrating the pressure with respect to density $\rho = N/V$ from the ideal gas limit. Alternatively, the potential decoupling procedure[9] for a single molecule, 1, say, may be employed. In this latter approach, the partially coupled molecule 1 is presumed to interact with its neighbors with potential $v(\mathbf{x}_1, \mathbf{x}_j; \xi)$, where

$$v(\mathbf{x}_1, \mathbf{x}_j; \xi = 0) \equiv 0 \tag{16}$$

represents full decoupling of 1, and

$$v(\mathbf{x}_1, \mathbf{x}_j; \xi = 1) = v(\mathbf{x}_1, \mathbf{x}_j)$$

is the actual "physical" pair potential, fully coupled. By computing the reversible work required to "switch on" $v(1, j; \xi)$, that is, to increase ξ from 0 to 1, one finds

$$\mu = \mu^{(0)} + kT\ln\left(\frac{N}{V}\right) + \frac{1}{N}\int_0^1 d\xi \int d\mathbf{x}_1 \int d\mathbf{x}_2 \frac{\partial v(\mathbf{x}_1, \mathbf{x}_2; \xi)}{\partial \xi} \rho^{(2)}(\mathbf{x}_1, \mathbf{x}_2; \xi) \tag{17}$$

The first two terms in the right member of (17) are the ideal gas contributions, and the integral term accounts for interactions. Note that $\rho^{(2)}$ must be suitably defined for a pair of particles, one of which displays the partial coupling feature.

The dielectric properties of polar fluids such as liquid water are intimately related to the orientational correlations between neighboring molecules. Kirkwood's theory of polar dielectrics[10] leads to the following expression for the static dielectric constant, ε_0:

$$\frac{(\varepsilon_0 - 1)(2\varepsilon_0 + 1)}{3\varepsilon_0} = \frac{4\pi N}{V}\left(\alpha + \frac{\mu_d^2 g_K}{3kT}\right) \tag{18}$$

where α is the molecular polarizability (assumed to be isotropic), and μ_d is

the permanent dipole moment. The specific form for orientational correlation, g_K, for water is again a pair-correlation function integral

$$g_K = 1 + \frac{N}{8\pi^2 V} \int d\mathbf{x}_2 (\mathbf{b}_1 \cdot \mathbf{b}_2) g^{(2)}(\mathbf{x}_1, \mathbf{x}_2) \tag{19}$$

and gives the average cosine of the angle between permanent dipole moment directions, $\mathbf{b}_1$ and $\mathbf{b}_2$, for neighboring molecules.

The definition of the hydrogen bond is somewhat arbitrary. Surely the various experimental techniques that are employed in its study are not precisely equivalent and need not quite agree on the concentration of hydrogen bonds in a given material sample. From our present point of view, we shall suppose that the existence of a "hydrogen bond" between two molecules of water means simply that their coordinates $\mathbf{x}_i$ and $\mathbf{x}_j$ lie between certain specified limits. This is equivalent to defining a characteristic bond function, $B(\mathbf{x}_i, \mathbf{x}_j)$, such that

$$B(\mathbf{x}_i, \mathbf{x}_j) = 1 \tag{20}$$

if i and j are so placed in space to form a hydrogen bond, and

$$B(\mathbf{x}_i, \mathbf{x}_j) = 0 \tag{21}$$

if not. Clearly B should be invariant to all but the relative positions and orientations of i and j. The average number, n_{HB}, of hydrogen bonds per molecule in water then is yet another example of a pair-distribution function quadrature

$$n_{\mathrm{HB}} = \frac{1}{2N} \int d\mathbf{x}_1 \int d\mathbf{x}_2 B(\mathbf{x}_1, \mathbf{x}_2) \rho^{(2)}(\mathbf{x}_1, \mathbf{x}_2) \tag{22}$$

Section 5 utilizes this general hydrogen-bond density expression with a specific set of B functions.

Finally, we note that the leading quantum-mechanical corrections to classical partition function (2), of order h^2, can also be reduced to pair-distribution function integrals. For the "asymmetric top" water molecule, the requisite expressions are quite complicated, and we refer the reader to a paper by Friedmann,[11] rather than reproducing the result here. Nevertheless it is worth pointing out that these quantum corrections are the key to understanding the small differences in equilibrium behavior of H_2O, D_2O, and T_2O.

3 Approximate Pair Potential

Our aim in this section is to exhibit a relatively compact analytical expression as an approximation to the "best" liquid-water pair potential. In doing so we are fully aware that our proposed form will eventually be supplanted

by more accurate approximations. Nevertheless it seems to us important to develop, even on the present rather crude basis, an intuitive grasp for the way water molecules in various orientations exert forces on one another. Since our proposed potential is forced to fit certain key experimental data, we feel that its predictions will ultimately prove not to be in serious quantitative error.

To the best of our knowledge, the only other type of pair potential that has seriously been considered in description of the fluid states of water is the Stockmayer potential.[12] This potential consists of a sum of a Lennard-Jones potential and the potential of interaction between permanent point dipoles. Doubtless this potential accurately portrays the interaction between pairs of water molecules at large distance in the dilute vapor. Indeed Rowlinson[13,14] has used the Stockmayer potential to calculate the second and third virial coefficients for water vapor.

Still, there is good reason to question the aptness of the Stockmayer potential for understanding condensed phases. It has, for example, been proven by Onsager[15] that the minimum energy for a set of point dipoles is attained in the hexagonal close-packed crystal, not the tetrahedrally coordinated ice lattice. (The Lennard-Jones potentials would merely add extra relative stability to the former.) Also, in the wide variety of hydrate crystals loosely termed "clathrates," the water molecules stoutly maintain the local tetrahedral coordination observed in ordinary ice, even though the larger geometric aspects of the water networks change considerably.[16]

We believe (consistent with Bernal and Fowler[3]) that the marked propensity for water molecules to hydrogen bond into networks with local tetrahedral coordination is the single most important observation bearing on selection of a suitable approximate pair potential. Therefore we have chosen for detailed consideration a model potential that manifestly favors tetrahedral coordination. Like the Stockmayer potential, it combines a spherically symmetric Lennard-Jones interaction with a noncentral electrostatic contribution. Instead of relying on point dipoles, though, our angle-dependent part is based on Bjerrum's four-point-charge model of the water molecule.[6]

As Figure 3 shows, these four charges are placed at the vertices of a regular tetrahedron whose center is presumed coincident with the oxygen nucleus. The distance from this center to each of the four charges has been chosen to be 1.00 Å. Two of the charges, with magnitude $+\eta e$, may be identified as the water-molecule protons partly shielded by the electron cloud. The remaining two charges, $-\eta e$, represent crudely the unshared pairs of valence-shell electrons in the molecule. Bjerrum has pointed out that the choice 0.17 for η will reproduce the dipole moment known for the free-water molecule, but owing to polarization effects in the liquid, we have elected to regard η as an adjustable parameter.

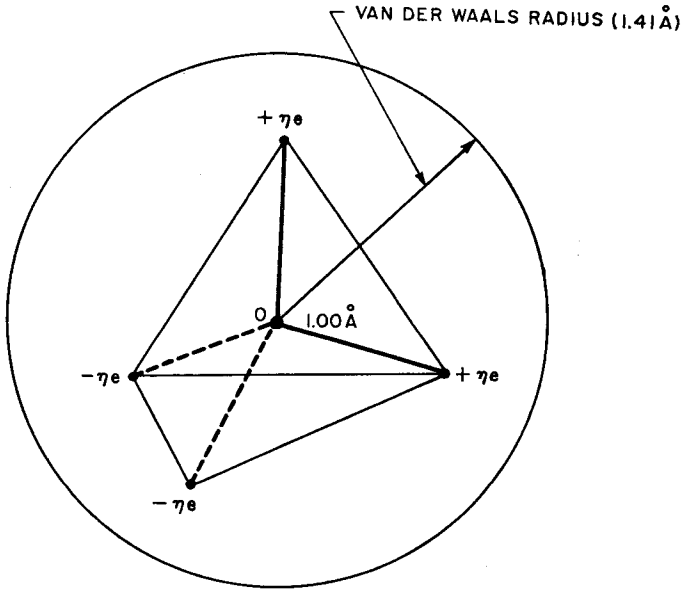

Figure 3. Tetrahedral charge distribution for the water molecule. The oxygen nucleus, 0, is at the center of the regular tetrahedron with circumradius 1.00 Å. The positive charge $+\eta e$, are shielded protons, and the negative charges simulate unshared electron pairs.

In order to avoid having simultaneously to determine a large number of adjustable parameters such as η, we have presumed that the Lennard-Jones 12,6 part is the same as for neon, which is isoelectronic with water

$$v_{LJ}(r_{12}) = 4\varepsilon\left[\left(\frac{\sigma}{r_{12}}\right)^{12} - \left(\frac{\sigma}{r_{12}}\right)^{6}\right]; \tag{23}$$

for neon[17]

$$\varepsilon = 5.01 \times 10^{-15}\ \text{erg} = 7.21 \times 10^{-2}\ \text{kcal/mole}, \qquad \sigma = 2.82\ \text{Å} \tag{24}$$

Specifically, v_{LJ} will refer to oxygen nuclei as the force centers. We see that the four Bjerrum charges $\pm\eta e$ are well buried inside the van der Waals radius (1.41 Å) of the molecule.

The electrostatic interaction between two tetrahedral charge distributions like the one shown in Figure 3 will consist of 16 separate charge-pair terms. It may be written thus

$$v_{el}(\mathbf{x}_1, \mathbf{x}_2) = (\eta e)^2 \sum_{\alpha_1,\alpha_2=1}^{4} \frac{(-1)^{\alpha_1+\alpha_2}}{d_{\alpha_1\alpha_2}(\mathbf{x}_1, \mathbf{x}_2)} \tag{25}$$

where α_1 and α_2, respectively, run over the four charges of molecules 1 and 2 such that even and odd values correspond to positive and negative charges.

The quantity $d_{\alpha_1\alpha_2}(\mathbf{x}_1, \mathbf{x}_2)$ is the scalar distance between the charges α_1 and α_2, and it obviously depends on the full set of molecular variables $\mathbf{x}_1$ and $\mathbf{x}_2$.

Except for one modification, the combination of (23) and (25) constitutes our water pair potential. The modification is required by the unphysical divergences that occur when two molecules move together in such a way that

$$d_{\alpha_1\alpha_2}(\mathbf{x}_1, \mathbf{x}_2) = 0 \tag{26}$$

Although this is not a serious matter when α_1 and α_2 have the same parity, it is catastrophic when they do not. For this reason, we multiply v_{el} by a "switching function," S, that is unity at large r_{12}, but vanishes when r_{12} is small enough that condition (26) might occur. Our complete water pair potential therefore has the form

$$v(\mathbf{x}_1, \mathbf{x}_2) = v_{LJ}(r_{12}) + S(r_{12})v_{el}(\mathbf{x}_1, \mathbf{x}_2) \tag{27}$$

The specific form utilized for the switching function consists of three separate parts

$$\begin{aligned} S(r_{12}) &= 0 && \text{for} \quad 0 \leq r_{12} \leq R_1 \\ &= \frac{(r - R_1)^2(3R_2 - R_1 - 2r)}{(R_2 - R_1)^3} && \text{for} \quad R_1 \leq r \leq R_2 \\ &= 1 && \text{for} \quad R_2 \leq r_{12} \leq \infty \end{aligned} \tag{28}$$

The cubic polynomial in interval $[R_1, R_2]$ renders $S(r_{12})$ a nondecreasing, continuous function with continuous first derivative. We must have $R_1 \geq 2.00$ Å to avoid the charge overlap catastrophe.

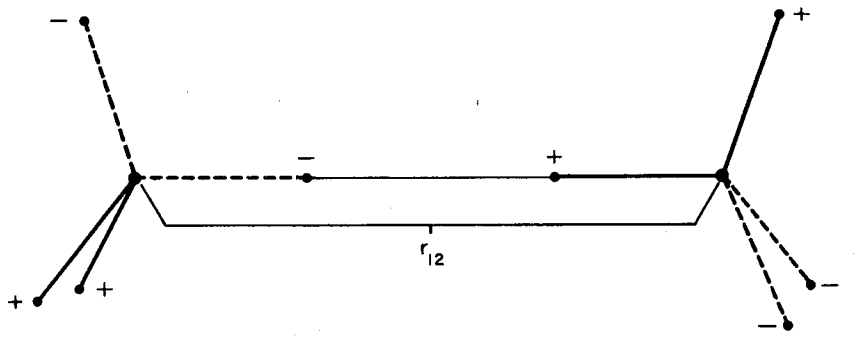

Figure 4. The symmetrical eclipsed (SE) approach of two water molecules. Looking down the "bond" axis, the two triads of charges not along this axis would seem to fall upon (or eclipse) one another.

Pair potential $v(\mathbf{x}_1, \mathbf{x}_2)$ contains three adjustable parameters, η, R_1, and R_2. These quantities were determined by requiring first, for fixed η, that the potential have a minimum in one of the nearest-neighbor pair configurations occurring in the ice lattice. The specific ice lattice configuration used is the "symmetrical eclipsed" configuration illustrated in Figure 4. We required that the minimum occur at $r_{12} = 2.76$ Å, the observed neighbor distance in ice. The value of $v(\mathbf{x}_1, \mathbf{x}_2)$ at that minimum was also fixed at several different trial values $v_{\min}$ so that the conditions

$$\begin{aligned} v(\mathbf{x}_1, \mathbf{x}_2)|_{2.76\,\text{Å}} &= v_{\min} \\ \frac{\partial v(\mathbf{x}_1, \mathbf{x}_2)}{\partial r_{12}}\bigg|_{2.76\,\text{Å}} &= 0 \end{aligned} \tag{29}$$

uniquely determined R_1 and R_2. The strategy was to choose $v_{\min}$ to provide a good fit to the water-vapor second virial coefficient, $B(T)$, computed by the method of Section 4.

It was not possible to reproduce the experimental $B(T)$ when η was preset at the Bjerrum value 0.17. Instead, it proved necessary to increase η to 0.19 to permit adequate fit. (This increase in η beyond the value of 0.17 may be ascribed to a polarization effect operative at small distances.) One then obtains

$$\begin{aligned} \eta &= 0.19 \\ R_1 &= 2.0379\,\text{Å} \\ R_2 &= 3.1877\,\text{Å} \end{aligned} \tag{30}$$

to complete the specification of $v(\mathbf{x}_1, \mathbf{x}_2)$. With this set of parameters, $v_{\min}$ for the symmetrical eclipsed, (SE), configuration is -6.50 kcal/mole, which is within the range of values quoted for hydrogen-bond energies.[18] Figure 5 presents the full r_{12} dependence of v in the SE configuration, along with the separate components v_{LJ}, S, and v_{el}.

Besides the SE configuration, there are three other nearest-neighbor configurations that occur in the ice lattice. They are illustrated in Figure 6. The nonsymmetrical eclipsed, NSE, configuration is obtained from SE by a 120° rotation about the oxygen–oxygen axis, and like SE its charges are in line with (i.e., eclipse) one another when viewed along this axis. The symmetrical staggered, SS, and nonsymmetrical staggered, NSS, cases have charges midway between one another when viewed along the oxygen–oxygen axis; SS is obtained from SE by a 180° rotation, and NSS from SE by a 60° rotation.

Figure 7 displays together the four potential curves, for varying r_{12}, for each of the ice configurations SE, NSE, SS, and NSS. The minima for the latter three numerically turn out to occur at the same distance, 2.76 Å, that

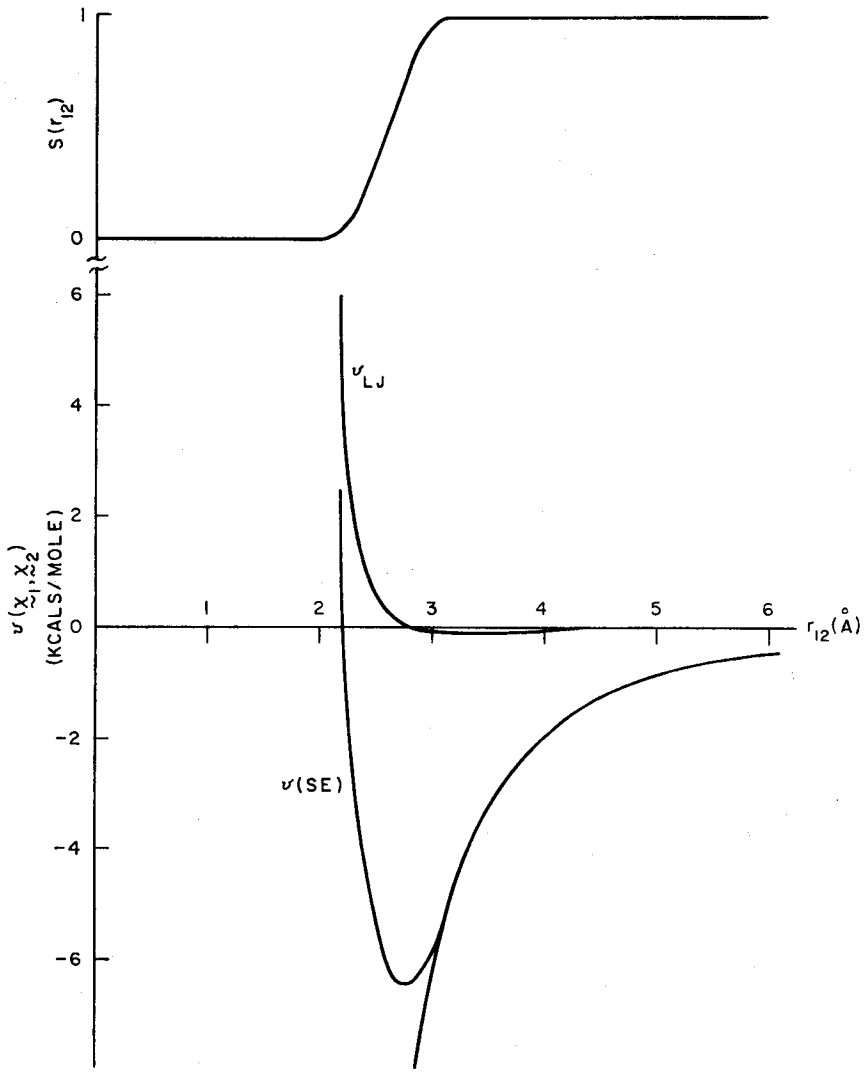

Figure 5. Potential curve for hydrogen bonding in the SE configuration; note three separate component functions v_{LJ}, S, and v_{el} related to $v(\mathbf{x}_1, \mathbf{x}_2)$ by (26).

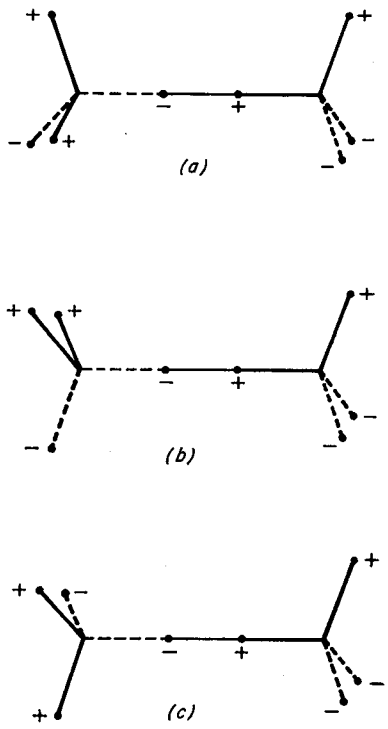

Figure 6. Ice-lattice neighbor configurations in addition to SE: (*a*) NSE; (*b*) SS; (*c*) NSS.

was forced upon the first one. However, the corresponding energies at those minima differ somewhat

$$\begin{aligned} &\text{SE} && -6.50 \text{ kcal/mole} \\ &\text{NSS} && -6.13 \text{ kcal/mole} \\ &\text{NSE} && -5.58 \text{ kcal/mole} \\ &\text{SS} && -5.34 \text{ kcal/mole} \end{aligned} \tag{31}$$

The numerical values of the curvatures $\partial^2 v/\partial r_{12}{}^2$ for each of the four potential curves, evaluated at the minima, are

$$\begin{aligned} v''(\text{SE}) &= 22.53 \text{ kcal/(mole)(Å}^2\text{)} \\ v''(\text{NSS}) &= 28.55 \text{ kcal/(mole)(Å}^2\text{)} \\ v''(\text{NSE}) &= 26.58 \text{ kcal/(mole)(Å}^2\text{)} \\ v''(\text{SS}) &= 25.78 \text{ kcal/(mole)(Å}^2\text{)} \end{aligned} \tag{32}$$

In the ice lattice, the staggered arrangements for nearest-neighbor pairs occur exactly three times as often as the eclipsed arrangements. Subject to

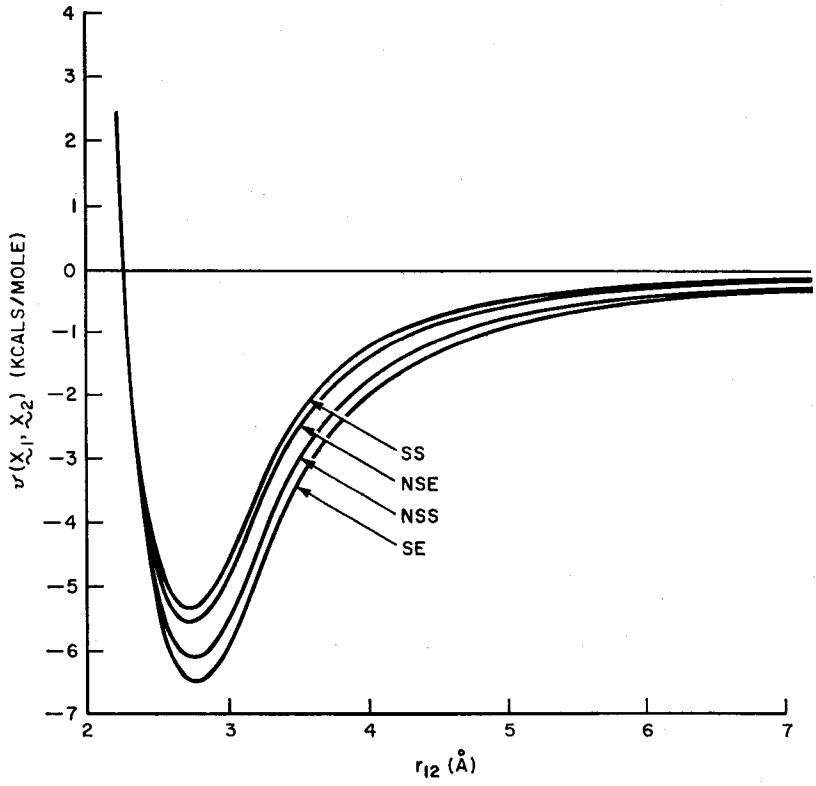

Figure 7. Potential curves for hydrogen bonding in the four ice lattice configurations.

this a priori restriction, Pauling's view of the residual entropy of ice[19] implies equal weights to the arrangements. We therefore calculate the "average curvature" to be

$$(v'')_{\text{av}} = \tfrac{1}{8}[v''(\text{SE}) + v''(\text{NSE})] + \tfrac{3}{8}[v''(\text{SS}) + v''(\text{NSS})] = 26.51 \text{ kcal/(mole)(Å}^2) \tag{33}$$

This average curvature may also be estimated from the measured isothermal compressibility of ice, found by Jona and Scherer[20] to be

$$\kappa_T = 1.11 \times 10^{-11} \text{ cm}^2/\text{dyne} \tag{34}$$

at $-16°$C. Assuming all nearest-neighbor distances to contract equally under compression, this κ_T is equivalent to

$$(v'')_{\text{av}} = 25.25 \text{ kcal/(mole)(Å}^2) \tag{35}$$

Actually, the neighbors with less potential curvature should move together more rapidly than the "stiffer" neighbors, hence tending to weight the former more. This might explain part of the discrepancy between (33) and (35).

On the basis of this rough comparison, we conclude that our water potential is not grossly in error for description of the condensed phases.

Several other potential curves have been computed for different classes of water molecule pair configurations. Figure 8 displays the results for a pair of "two-bonded" configurations, TB_1 and TB_2; for both of these, two pairs of opposite charges simultaneously approach one another. Nevertheless, the distances involved are such that the repulsive part of v_{LJ} comes into play before the charge attractions get very large, so the net potential at the two-bonded minima is considerably higher than the single-bond results in (31). It therefore seems quite unlikely that two-bonded configurations play any significant role in liquid water.

Several structural models for liquid water, such as those proposed by Pauling,[21] Frank and Quist,[22] and Samoilov,[23] postulate the existence of

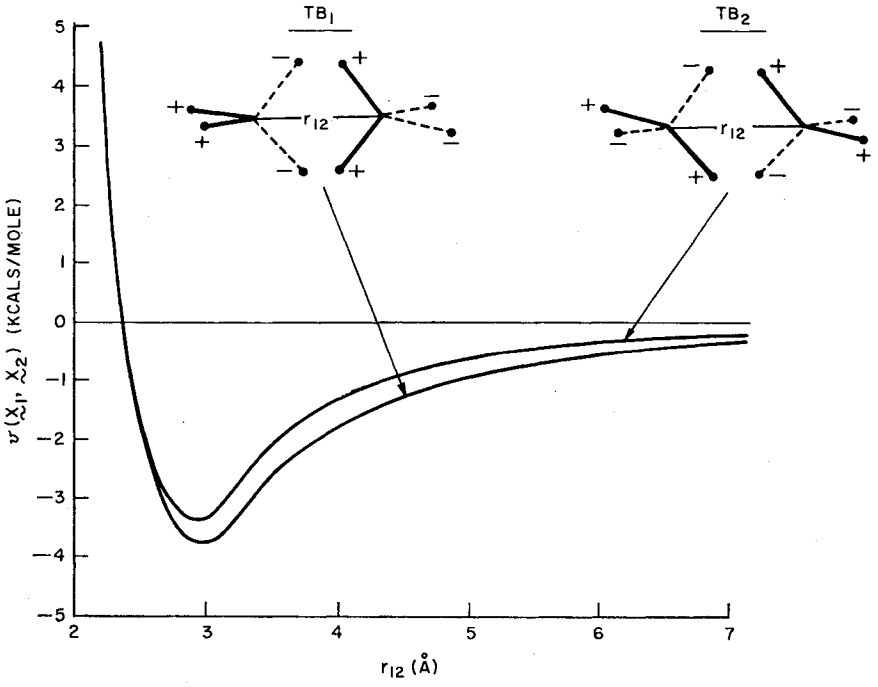

Figure 8. Potential curves for "two-bonded" configurations.

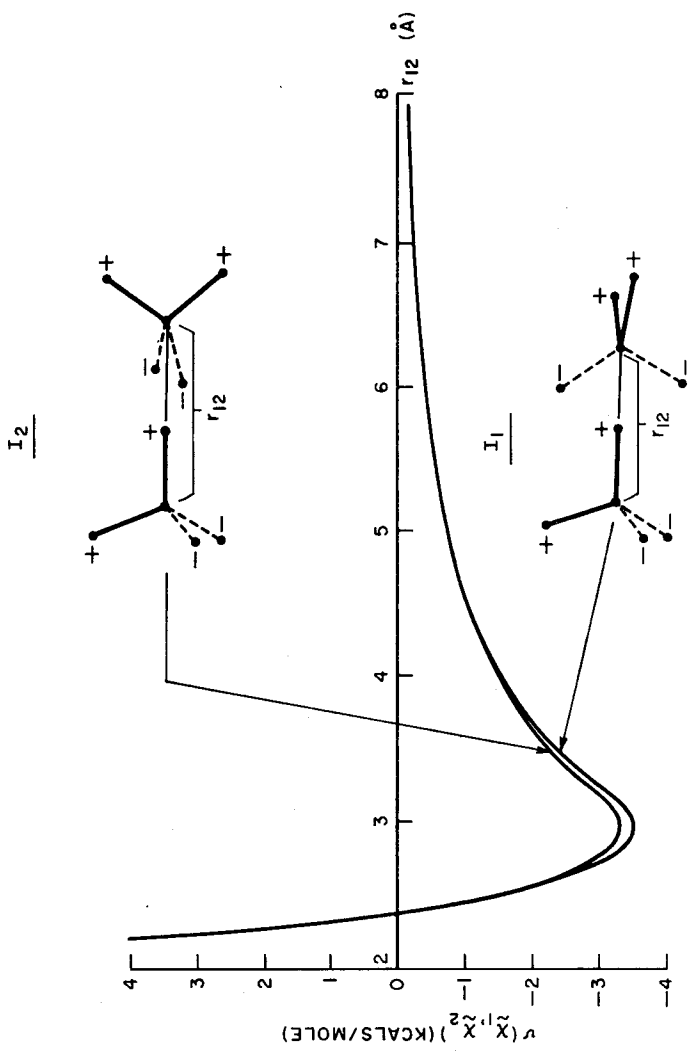

Figure 9. Two "interstitial" configuration potential curves. For both, the interstitial "monomer" molecule approaches the "lattice" molecule along the direction of the latter's permanent dipole moment. I_1 and I_2 differ by a 90° rotation.

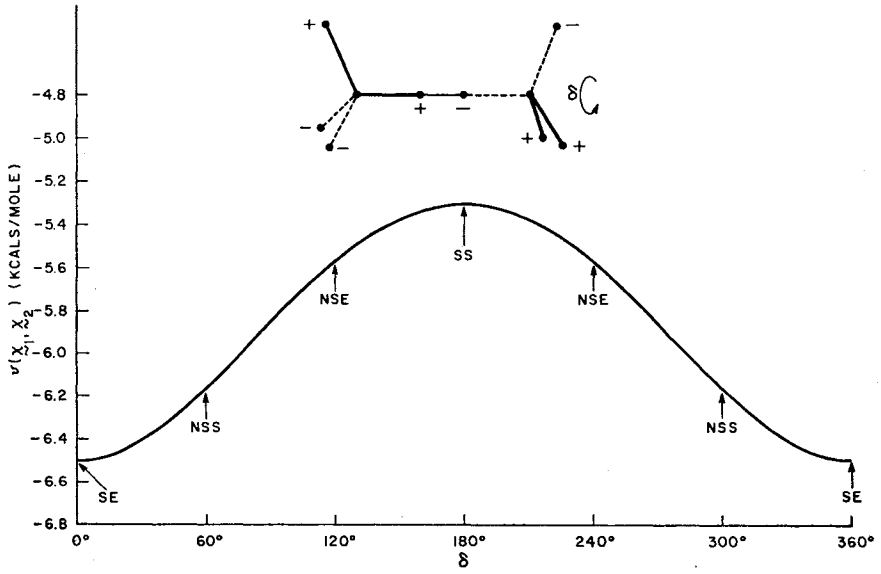

Figure 10. Rotational potential for two water molecules, with $r_{12} = 2.76$ Å. As angle δ increases from 0, the SE configuration deforms first to NSS ($\delta = 60°$), then to NSE (120°), and then SS ($\delta = 180°$). The curve is symmetric at about $\delta = 180°$.

"monomeric interstitial" water molecules, trapped in cavities formed by hydrogen-bonded lattices. It is therefore pertinent to calculate potential curves for one molecule (the monomer) approaching another (a member of the lattice) along directions expected from the interstitial picture. Figure 9 presents two such curves. Again we see that the energy is substantially higher at the minima than for the four ice-lattice configurations, SE, NSE, SS, NSS. Nevertheless, such interstitial molecules can be somewhat stabilized by relatively free rotation.

Figure 10 exhibits a rotational potential energy curve. The two molecules start in the SE configuration, with $r_{12} = 2.76$ Å, and are rotated about the oxygen–oxygen axis. This process produces in turn the following sequence of configurations during a full 360° rotation: SE, NSS, NSE, SS, NSE, NSS, SE.

Finally, Figure 11 provides the predicted potential energy curve for a particular hydrogen-bond bending mode. This bend (also performed at fixed $r_{12} = 2.76$ Å) carries SE continuously to SS through a substantial potential barrier. From Figure 9, we see that the top of the barrier corresponds to interstitial configuration, I_1.

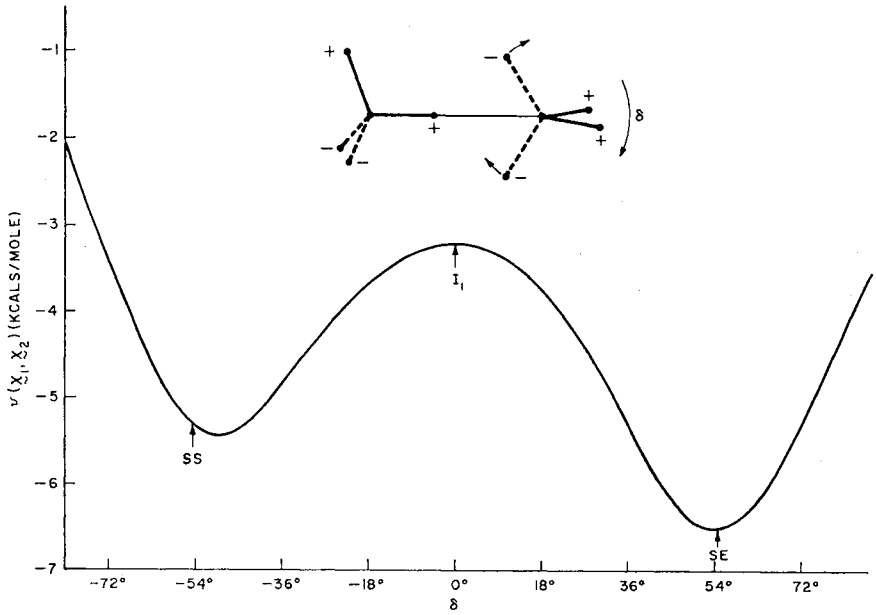

Figure 11. Potential curve for hydrogen-bond "bending," with r_{12} fixed at 2.76 Å. Configurations SS and SE occur at one-half the ideal tetrahedral angle, or 54.7°.

A survey of the various potential curves indicates that the absolute minimum potential energy for two water molecules is predicted by approximation (27) to occur at very nearly the geometrically ideal SE configuration, with $r_{12} \simeq 2.76$ Å.

4 Virial Coefficients

In the low-density vapor phase, the pressure equation of state (13) may be expanded into a density series

$$\frac{pV}{NkT} = 1 + B(T)\left(\frac{N}{V}\right) + C(T)\left(\frac{N}{V}\right)^2 + D(T)\left(\frac{N}{V}\right)^3 + \cdots \tag{36}$$

The second, third, fourth,..., virial coefficients (B, C, D,..., respectively) convey the extent of imperfection of the gas, and they are intimately related to the interactions among clusters of ascending numbers of molecules.

The specific statistical-mechanical expressions for the virial coefficients in (36) may be obtained from (13) by insertion of an appropriate density series

for $\rho^{(2)}(\mathbf{x}_1, \mathbf{x}_2)$, followed by partial integrations. However, a more direct route to the same results is provided by the standard Mayer cluster theory.[24] The second virial coefficient has the form

$$B(T) = -\frac{1}{16\pi^2}\int d\mathbf{x}_2 \{\exp[-\beta v(\mathbf{x}_1, \mathbf{x}_2)] - 1\} \tag{37}$$

Knowledge of the total temperature dependence of $B(T)$ obviously does not in itself permit complete determination of $v(\mathbf{x}_1, \mathbf{x}_2)$. However, this knowledge can be useful in fixing free parameters in an assumed analytical approximation. On account of the exponential character of the integrand in (37), the value of $B(T)$ measured at low temperature is especially helpful in fitting $v(\mathbf{x}_1, \mathbf{x}_2)$ near its absolute minimum.

Reference to (3) shows that $B(T)$ for water is a sixfold integral. It is therefore much more difficult to evaluate with comparable accuracy than the single integration required for argon, the archetypal structureless spherical molecule. Still, methods have been developed for numerical integration of expressions such as (37); examples are the Haselgrove[25] and Conroy[26] techniques.

The few configurations for which the water pair potential was evaluated in the previous section were sufficiently special that convenient expressions could be written out, for computational purposes, for the charge-charge distance $d_{\alpha_1\alpha_2}$ in v_{el}. But regardless of the specific integration scheme to be used for $B(T)$, it is necessary to evaluate $v(\mathbf{x}_1, \mathbf{x}_2)$ for very many configurations, the majority of which are irregular. For that reason we were compelled to develop a computer-coded system for finding v, given an arbitrary $\mathbf{x}_1$ and $\mathbf{x}_2$. This procedure utilizes transformation matrices $\mathbf{E}(\phi_i, \theta_i, \psi_i)$, depending on Euler angles for molecule i, which convert any vector $\mathbf{t}$ in the laboratory coordinate system, to the same vector $(\mathbf{t})^{(i)}$ resolved into components parallel to the right-handed coordinate system ($\mathbf{b}$, $\mathbf{m}$, $\mathbf{n}$ in Figure 1) attached to molecule i

$$(\mathbf{t})^{(i)} = \mathbf{E}(\phi_i, \theta_i, \psi_i)\cdot\mathbf{t} \tag{38}$$

Since we have

$$\begin{aligned} d^2_{\alpha_1\alpha_2} &= [\mathbf{r}_{12} + \mathbf{t}_{\alpha_2} - \mathbf{t}_{\alpha_1}]^2 \\ &= r_{12}^2 + \mathbf{t}_{\alpha_2}^2 + \mathbf{t}_{\alpha_1}^2 + 2\mathbf{r}_{12}\cdot\mathbf{t}_{\alpha_2} - 2\mathbf{r}_{12}\cdot\mathbf{t}_{\alpha_1} - 2\mathbf{t}_{\alpha_1}\cdot\mathbf{t}_{\alpha_2} \end{aligned} \tag{39}$$

where $\mathbf{t}_{\alpha_1}$ and $\mathbf{t}_{\alpha_2}$ are the displacements of charges α_1 and α_2 relative to their respective oxygen nuclei, it follows that

$$\begin{aligned} d^2_{\alpha_1\alpha_2} = {} & r_{12}^2 + \mathbf{t}_{\alpha_2}^2 + \mathbf{t}_{\alpha_1}^2 + 2\mathbf{r}_{12}\cdot[\mathbf{E}^{-1}(2)\cdot(\mathbf{t}_{\alpha_2})^{(2)} - \mathbf{E}^{-1}(1)\cdot(\mathbf{t}_{\alpha_1})^{(1)}] \\ & - 2[\mathbf{E}^{-1}(1)\cdot(\mathbf{t}_{\alpha_1})^{(1)}]\cdot[\mathbf{E}^{-1}(2)\cdot(\mathbf{t}_{\alpha_2})^{(2)}] \end{aligned} \tag{40}$$

The charge-position vectors, $(\mathbf{t}_{\alpha_i})^{(i)}$, can all easily be expressed in terms of the unit vectors **b**, **m**, and **n**, so that the matrices $\mathbf{E}^{-1}$ in (40) account for arbitrary molecular rotations.

The Haselgrove method was actually the one used in our $B(T)$ calculations because it permits use of varying numbers of points, thus allowing estimation of integration error. For $0 \leq r_{12} \leq 2.00$ Å, the integrand shown in (37) is essentially constant at -1, so the contribution from this range to $B(T)$ is trivial to take into account. The actual numerical integration therefore was restricted to the range

$$2.00 \text{ Å} \leq r_{12} \leq 15.00 \text{ Å} \tag{41}$$

since for larger separations the contributions are negligible. Typical computations at a given temperature involve 12,000 distinct pair configurations.

Table 1 shows the values computed for $B(T)$. We estimate the error to be about 5%. For comparison the table also includes Rowlinson's results for the Stockmayer potential,[13] as well as Kell, McLaurin, and Whalley's recent measurements.[27] As explained in Section 3, it was necessary to try different values of the charge magnitudes $\pm\eta e$. The numbers quoted in the table refer to $\eta = 0.19$.

Table 1 Second Virial Coefficient for Water (cm^3/mole)

Temperature (°C)	$B(T)$[a]	Stockmayer Potential (Ref. 13)	Experiment (Ref. 27)
100	−466	−450	−450[b]
200	−190	−205	−197
300	−107	−122	−112
400	−65	−80	−72

[a] Computed from (37), using pair potential (27).
[b] Extrapolated from 150°C.

When η was preset as low as 0.17 (the Bjerrum value), and $v_{\min}$ varied, it was not possible to fit the experimental $B(T)$. The error was most significant at low T, and reflected too weak an attraction. On the other hand, when η was increased substantially beyond 0.19, it became impossible to find R_1 and R_2 to satisfy (29). The value chosen for η therefore seemed to represent a satisfactory intermediate value.

It would be unwarranted at this stage to spend a considerable effort to improve agreement between the theoretical and experimental $B(T)$'s. Surely this eventually could be done by a combination of the following: (a) shifts in

positions of the charges from the regular tetrahedron vertices, (b) change in shape of the switching function, and (c) variation of ε and σ in v_{LJ} from the neon values.

But even if numerical error in integration of $B(T)$ were to be made negligibly small, one would still be confronted by quantum corrections and by the fact that the best pair potential for the liquid state, our primary object of interest here, very likely deviates somewhat from the true pair potential for isolated molecules. We believe, however, that our approximate fit to the experimental $B(T)$ serves to force upon $v(\mathbf{x}_1, \mathbf{x}_2)$ in (27) nearly the correct energy for hydrogen-bond formation. Since the fits to the measured $B(T)$ obtained with both our potential and the Stockmayer potential are about equally good, we see how insensitive $B(T)$ is to angular variations, and this serves to stress the importance of seeking other information to determine those angular variations.

The analog of $B(T)$ expression (37) for the third virial coefficient is a twelvefold integral

$$
\begin{aligned}
C(T) = &-\frac{1}{3(8\pi^2)^2} \\
&\times \int d\mathbf{x}_2 \int d\mathbf{x}_3 \{\exp[-\beta V_3(\mathbf{x}_1, \mathbf{x}_2, \mathbf{x}_3)] \\
&\quad -\exp[-\beta(v(\mathbf{x}_1, \mathbf{x}_2) + v(\mathbf{x}_2, \mathbf{x}_3))] \\
&\quad - \exp[-\beta(v(\mathbf{x}_1, \mathbf{x}_2) + v(\mathbf{x}_1, \mathbf{x}_3))] \\
&\quad - \exp[-\beta(v(\mathbf{x}_1, \mathbf{x}_3) + v(\mathbf{x}_2, \mathbf{x}_3))] \\
&\quad + \exp[-\beta v(\mathbf{x}_1, \mathbf{x}_2)] + \exp[-\beta v(\mathbf{x}_1, \mathbf{x}_3)] \\
&\quad + \exp[-\beta v(\mathbf{x}_2, \mathbf{x}_3)] - 1\}
\end{aligned} \tag{42}
$$

In the event that the three-molecule potential energy, V_3, is composed just of pair potential contributions, the $C(T)$ expression simplifies considerably

$$
C(T) = -\frac{1}{3(8\pi^2)^2} \int d\mathbf{x}_2 \int d\mathbf{x}_3 \, f(\mathbf{x}_1, \mathbf{x}_2) f(\mathbf{x}_1, \mathbf{x}_3) f(\mathbf{x}_2, \mathbf{x}_3) \tag{43}
$$

where

$$
f(\mathbf{x}_i, \mathbf{x}_j) = \exp[-\beta v(\mathbf{x}_i, \mathbf{x}_j)] - 1 \tag{44}
$$

The third virial coefficient is very sensitive to intermolecular potentials because it involves cancellation between large positive and large negative contributions coming from different regions of triplet configuration space.

It is much more difficult to carry out the integrations demanded for $C(T)$, even numerically, than for $B(T)$. Even so, we thought it worthwhile to seek a rough evaluation of $C(T)$ for comparison with experiment. Conroy's

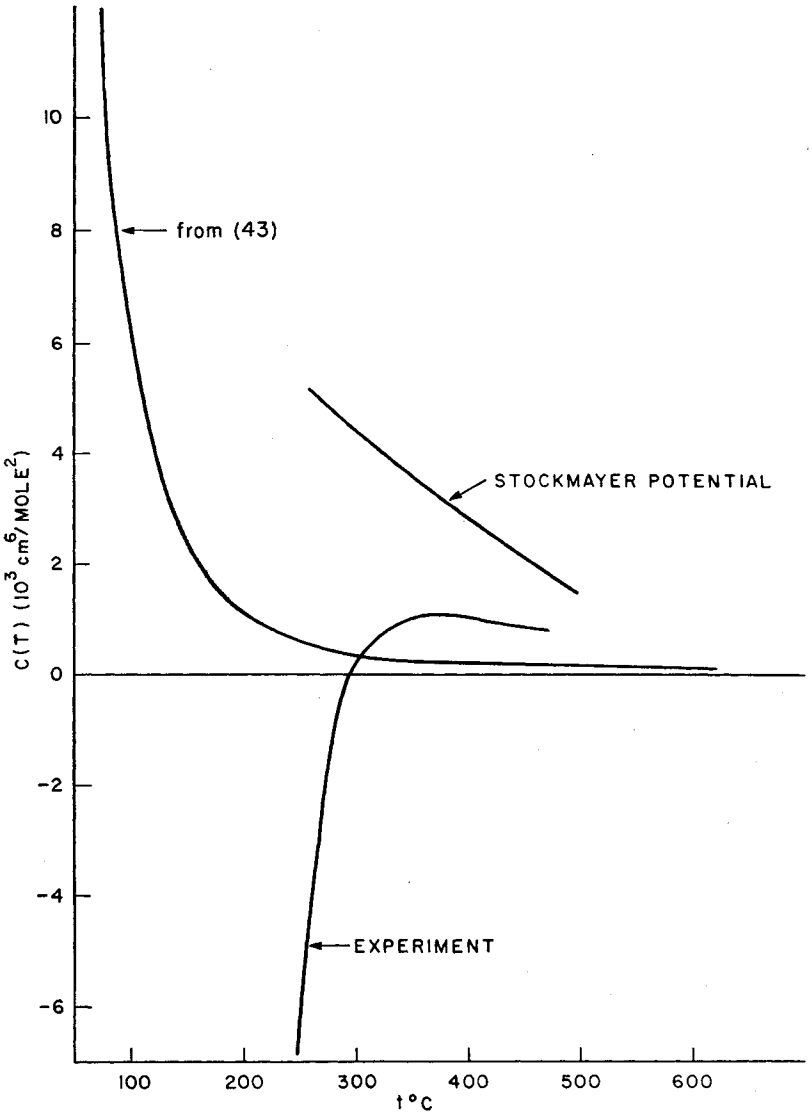

Figure 12. Third virial coefficient for water: the theoretical curve based on $C(T)$ expression (43) uses pair potential (27).

numerical integration procedure[26] was employed using potential (27) in (43). This procedure involved consideration of 9644 separate triplet configurations. The results (probably only accurate within a factor of 2) are presented in Figure 12, along with Rowlinson's Stockmayer potential $C(T)$,[14] as well as Kell, McLaurin, and Whalley's experimental values.[27]

It is clear that neither the Stockmayer potential nor our present form in (27) comes anywhere near to predicting an experimentally acceptable $C(T)$. The chief source of error is probably the fact that V_3 in general $C(T)$ expression (42) is not precisely a sum of v's for the separate pairs, but contains as well a true three-body potential. This inherent three-body part should consist mainly of a polarization effect; that is, one molecule interacts with the dipole moment induced in a second one by the third. Even though the extra three-body energy may be small, its effect can be very large, for it acts as a multiplier for

$$\exp\{-\beta[v(\mathbf{x}_1, \mathbf{x}_2) + v(\mathbf{x}_1, \mathbf{x}_3) + v(\mathbf{x}_2, \mathbf{x}_3)]\} \tag{45}$$

to form the first integrand term in (42). If the three molecules are arranged to form two SE hydrogen bonds, with energy -13 kcal/mole, (45) at room temperature is about 2×10^9, and one of the succeeding integrand terms in (42) will have comparable magnitude but opposite sign. With such huge numbers, $C(T)$ ends up being exceedingly sensitive to inclusion of very small three-body potentials.

Although a refinement of our water pair potential might improve agreement in Figure 12 somewhat, it should be stressed that prediction of a $C(T)$ in close agreement with experiment is not a prerequisite to formulation of an adequate liquid-state theory.

5 Pair-Correlation Function

We turn now to survey some theoretical aspects of the water pair-correlation function. This quantity may be expressed as

$$g^{(2)}(\mathbf{x}_1, \mathbf{x}_2) = \exp\{-\beta[v(\mathbf{x}_1, \mathbf{x}_2) + w(\mathbf{x}_1, \mathbf{x}_2)]\} \tag{46}$$

The function w is both temperature and density dependent, and it comprises the average influence of the water medium surrounding fixed molecules 1 and 2.

In the large-r_{12} limit, of course, both the direct interaction, v, as well as the indirect correlation quantity, w, will vanish, to give unity for $g^{(2)}$. However, we can also specify the precise way in which $v + w$ goes to 0, because at large distances only the molecular dipole moments interact. Neglecting

molecular polarizability, we see that molecule 1 will be surrounded by a polarization field at large distance equal to

$$\mathbf{P}_1 = \frac{\varepsilon_0 - 1}{4\pi} \mathbf{E}_1 \tag{47}$$

where $\mathbf{E}_1$ is the electric field due to molecule 1 and its orientationally correlated near neighbors. Classical electrostatics subsequently gives the following expression for $\mathbf{E}_1$[10]

$$\mathbf{E}_1(\mathbf{r}_{12}) = -\frac{3\mu_d g_K}{2\varepsilon_0 + 1} \nabla_2 \frac{\mathbf{b}_1 \cdot \mathbf{r}_{12}}{r_{12}^3} \tag{48}$$

If this is substituted into (47) and the result identified as a deviation from isotropy of the distribution of directions for vector $\mathbf{b}_2$ in molecule 2, we must have

$$\beta[v(\mathbf{x}_1, \mathbf{x}_2) + w(\mathbf{x}_1, \mathbf{x}_2)] \sim \frac{9 g_K(\varepsilon_0 - 1)}{4\pi\rho(2\varepsilon_0 + 1)} \mathbf{b}_1 \cdot \mathbf{T}_{12} \cdot \mathbf{b}_2 \tag{49}$$

where $\mathbf{T}_{12}$ is the dipole-dipole tensor

$$\mathbf{T}_{12} = \frac{1}{r_{12}^3} \left(\mathbf{1} - \frac{3\mathbf{r}_{12}\mathbf{r}_{12}}{r_{12}^2} \right) \tag{50}$$

In the low-density limit applicable to water vapor, w vanishes, so that the pair-correlation function, $g^{(2)}$, reduces to the Boltzmann factor for direct interaction, v

$$\lim_{\rho \to 0} g^{(2)}(\mathbf{x}_1, \mathbf{x}_2) = \exp\left[-\beta v(\mathbf{x}_1, \mathbf{x}_2)\right] \tag{51}$$

The simpler correlation function $\bar{g}^{(2)}(r_{12})$, also in the zero-density limit, is equal to an angular average of (51)

$$\lim_{\rho \to 0} \bar{g}^{(2)}(r_{12}) = \frac{1}{(8\pi^2)^2} \int \sin\theta_1 \, d\phi_1 \, d\theta_1 \, d\psi_1 \int \sin\theta_2 \, d\phi_2 \, d\theta_2 \, d\psi_2 \times \exp\left[-\beta v(\mathbf{x}_1, \mathbf{x}_2)\right] \tag{52}$$

This quantity gives the relative density of oxygen nuclei (regardless of molecular orientations) at distance r_{12} from the oxygen nucleus of a fixed molecule in the dilute vapor.

With the specific interaction (27), the integral in (52) has been evaluated at 4°C, and the result is plotted in Figure 13. The very high peak at about the ice-lattice spacing (2.76 Å) reflects the very strong attraction due to hydrogen bonding when the molecules are suitably oriented. Although the function has the same qualitative features as the pair Boltzmann factor for, say, a pair of argon atoms, the peak height is very much larger than for argon at the corresponding temperature. (The maximum of $\exp[\beta v_{LJ}(r)]$ for argon at

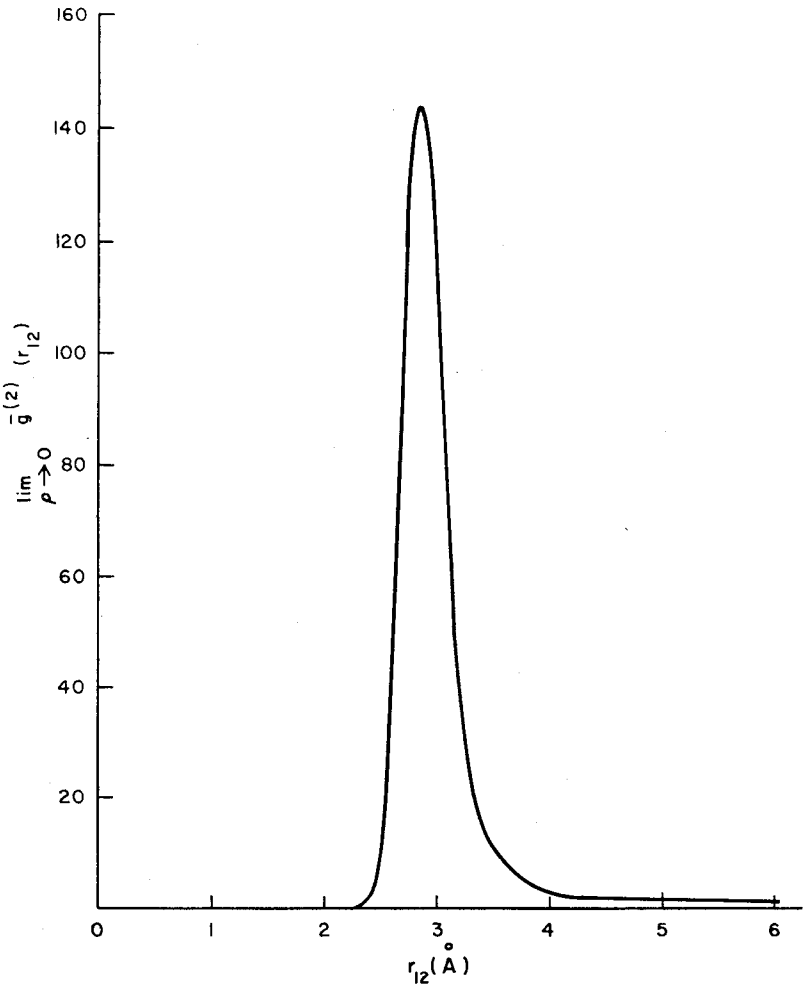

Figure 13. Low-density limit for $\bar{g}^{(2)}(r_{12})$ at 4°C.

83.8°K, its triple-point temperature, is only about 4.2.) Even in this orientationally averaged sense, we see that liquid water must be regarded as an extremely strongly interacting many-body system.

One of the more important trends in liquid-state theory in recent years has been the development of integral equation techniques for prediction of pair-correlation functions.[5] So far, this approach has been applied numerically only to fluids composed of spherical structureless particles, but it is important to establish the extent of its possible utility for water. By most measures, the

Percus–Yevick integral equation[28] is the most reliable of those available; for water it is

$$\exp[\beta v(\mathbf{x}_1, \mathbf{x}_2)] g^{(2)}(\mathbf{x}_1, \mathbf{x}_2) = 1 + \frac{N}{8\pi^2 V} \int d\mathbf{x}_3 [g^{(2)}(\mathbf{x}_1, \mathbf{x}_3) - 1] \times \{1 - \exp[\beta v(\mathbf{x}_3, \mathbf{x}_2)]\} g^{(2)}(\mathbf{x}_3, \mathbf{x}_2) \tag{53}$$

The speed and memory capacity of modern computers has reached a point where iterative solution of the Percus–Yevick equation for simple fluids such as argon is a relatively simple task.[29] However, it has already been pointed out that the water $g^{(2)}$ is a function of no less than six variables, rather than just radial distance as for simple fluids. It should be mentioned parenthetically, that one of the two molecules may be regarded as fixed in position and orientation. The six variables may then be taken to be the three polar coordinates of oxygen nucleus 2 relative to 1, and the three Euler angles for molecule 2. The corresponding numerical task for water, therefore, is orders of magnitude more difficult. To convey the structural information implicit in $g^{(2)}(\mathbf{x}_1, \mathbf{x}_2)$, a minimum of about 10 discrete values for each of the six variables should be considered, thus requiring a table of one million entries!

Also, our experience with trial integrals has shown that about four minutes is required to carry out the integral in (53), for each pair-configuration $\mathbf{x}_1$, $\mathbf{x}_2$, with even modest numerical accuracy. Therefore each iteration of (53) in seeking a numerical $g^{(2)}$ for water would require more than one thousand hours of computing time! Similar estimates apply to the other integral equations currently in vogue, so the difficulty is not to be regarded as a special intractability of the Percus–Yevick equation.

In spite of the present virtual impossibility of solving the Percus–Yevick integral equation (or any of the others) for liquid water, this general approach can still provide some indirect insight. For example, we can observe the effect on local structure of the hydrogen-bonding part of $v(\mathbf{x}_1, \mathbf{x}_2)$ by first integrating the Percus–Yevick equation with just the first term in the potential expression (27), and then comparing the result with the *experimental* $\bar{g}^{(2)}(r_{12})$. Figure 14 shows the two curves together, and both refer to 4°C, and the 1-atm molecular density for real water. The theoretical curve represents highly compressed, supercritical neon gas (the pressure would be about 5000 atm), since with only central interactions operative the molecular rotations are free and irrelevant. The experimental curve was determined by Narten, Danford, and Levy;[30] it probably contains slight artifacts (from Fourier inversion of the scattering data) such as the bump at 3.7 Å.

Not only does the hydrogen-bond part (Sv_{el}) of the water pair potential cause an enormous pressure reduction from 5000 to 1 atm, but we also see that the first peak of the pair-correlation function undergoes very marked narrowing. As a result, the number of nearest neighbors, defined by the area under

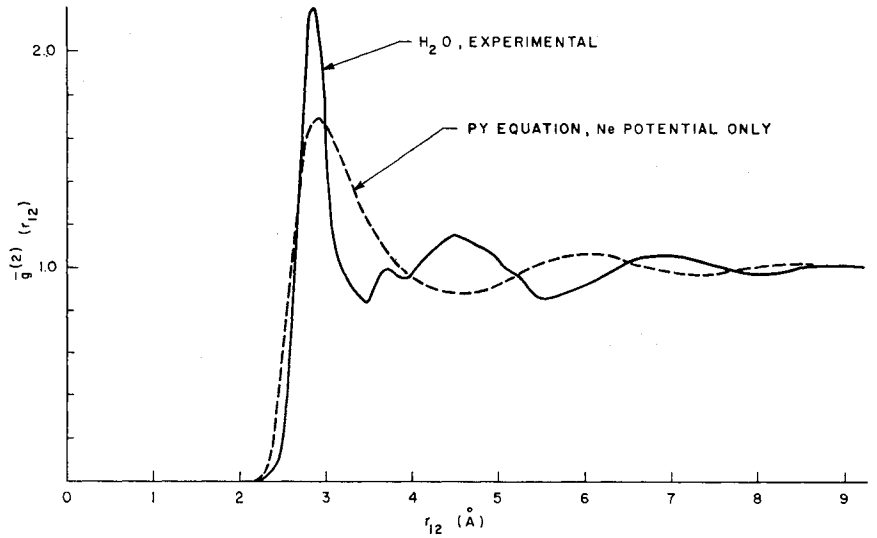

Figure 14. Comparison of the experimental $\bar{g}^{(2)}$ for water at 4°C, with the radial distribution function calculated from the Percus–Yevick equation (same temperature and density) using only the Lennard-Jones part of water potential (27).

the first peak out to the subsequent minimum, reduces from around eight for neon to roughly four for water.

Figure 14 also shows that the first-peak narrowing is accompanied by inward movement of the subsequent $\bar{g}^{(2)}(r_{12})$ peaks, so that the oscillations about the first peak for neon and for water are "out of phase." In the neon case, the second and third peaks are very nearly at two and three times the first-peak distance, respectively. Although the second peak for water is quite broad, its maximum lies very close to the position expected for perfect tetrahedral coordination, namely, $2 \sin (54°44') \simeq 1.633$ times the first-peak distance. The third water peak is too diffuse to identify uniquely and likely represents contributions from a wide variety of local structures that are possible with predominantly tetrahedral linkage.

The function $w(\mathbf{x}_1, \mathbf{x}_2)$ in (46), the general expression for the water pair-correlation function, may in principle be expanded in some complete orthonormal set of functions, F_α, of just the Euler angle variables

$$w(\mathbf{x}_1, \mathbf{x}_2) = w_0(r_{12}) + \sum_{\alpha=1}^{\infty} w_\alpha(r_{12}) F_\alpha(\phi_1 \cdots \psi_2) \tag{54}$$

where the coefficient functions, w_α, depend only on r_{12}. Equation 49 indicates the behavior of this expansion at large r_{12}, but greater structural significance

attaches to the case of small r_{12}, when the molecules are first, second, or third neighbors, roughly. For such close pairs, the direct pair potential $v(\mathbf{x}_1, \mathbf{x}_2)$ exerts very strong forces and torques, and it is unclear what relative importance the angle-dependent ($\alpha \geq 1$) parts of $w(\mathbf{x}_1, \mathbf{x}_2)$ would have. In order to get some information on this point, we shall tentatively disregard the α sum in (54), and observe the consequences. We therefore assume for the moment that

$$g^{(2)}(\mathbf{x}_1, \mathbf{x}_2) \simeq y(r_{12}) \exp\left[-\beta v(\mathbf{x}_1, \mathbf{x}_2)\right] \tag{55}$$

where

$$y(r_{12}) = \exp\left[-\beta w_0(r_{12})\right] \tag{56}$$

If (55) is averaged over Euler angles $\phi_1 \cdots \psi_2$ at fixed r_{12}, the result is

$$\bar{g}^{(2)}(r_{12}) = y(r_{12}) \lim_{\rho \to 0} \bar{g}^{(2)}(r_{12}) \tag{57}$$

The left-hand member is the measured radial correlation function (shown in Figure 14), and the zero-density limit appearing in the right-hand member has already been computed and displayed in Figure 13. We can therefore combine these two pieces of information to produce a semiempirically determined $y(r_{12})$, which is shown in Figure 15. The most important feature of $y(r_{12})$ is its small value ($\simeq 0.015$) at the nearest-neighbor distance; this value prevents more than about four neighbors from fitting around any one molecule.

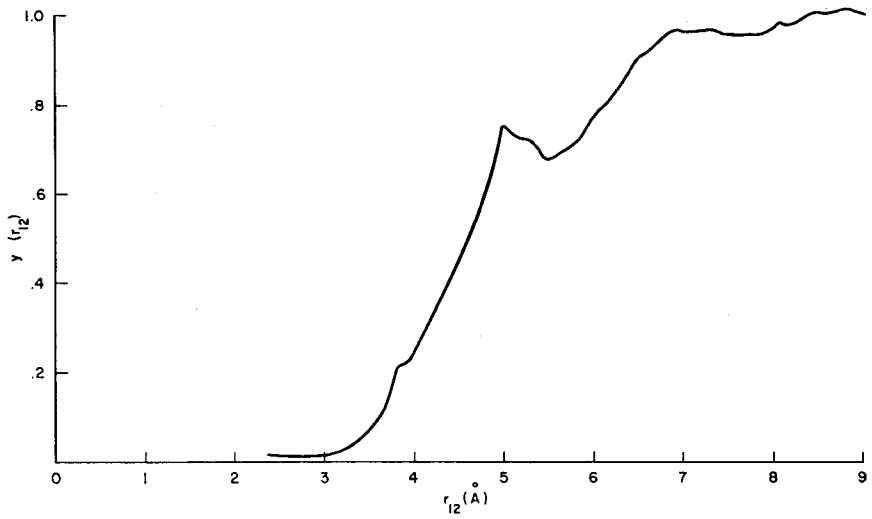

Figure 15. Semiempirically determined $y(r_{12})$ for water at 4°C and 1 atm. For r_{12} less than 2.5 Å, relation (57) for computing $y(r_{12})$ becomes effectively indeterminate.

Now that $y(r_{12})$ has been determined, it may be used in (55) along with our pair potential, (27), to yield an approximate pair-correlation function. The latter then may be utilized in (19) to calculate an approximate dielectric g_K. The result for water at 4°C is

$$g_K = 1.94 \tag{58}$$

On the other hand, Harris, Haycock, and Alder[31] have shown that g_K must be about 2.6 to be consistent with the measured dielectric constant. We are therefore forced to conclude that approximation (55) fails to give a proper account of orientational correlation between neighboring water molecules; in other words, it produces too little angular correlation.

This conclusion may be confirmed by calculating the number of hydrogen bonds per molecule n_{HB}, from (22), again employing the approximate water $g^{(2)}$ in (55). By "hydrogen bond" between two molecules, we shall mean that the pair potential for them shall be less than some preassigned upper limit, u. In other words, the characteristic bond function $B(\mathbf{x}_1, \mathbf{x}_2)$ may be written

$$B(\mathbf{x}_1, \mathbf{x}_2) = U[u - v(\mathbf{x}_1, \mathbf{x}_2)] \tag{59}$$

where

$$\begin{aligned} U(s) &= 0 \qquad s < 0 \\ &= 1 \qquad s \geq 0 \end{aligned} \tag{60}$$

is the unit step function. Table 2 presents the values calculated in this way for n_{HB} in 4°C water at 1-atm pressure.

Table 2 Number of Hydrogen Bonds per Water Molecule, n_{HB}, as the Cutoff Energy, u, is varied[a]

u (kcal/mole)	n_{HB}
−4.75	7.0×10^{-1}
−5.00	5.0×10^{-1}
−5.25	3.4×10^{-1}
−5.50	2.1×10^{-1}
−5.75	1.0×10^{-1}
−6.00	1.8×10^{-2}
−6.25	3.0×10^{-3}
−6.45	4.1×10^{-5}

[a] Pair-correlation function provided by (55); 4°C and 1 atm.

As u moves downward toward -6.50 kcal/mole, the number of hydrogen bonds per molecule declines rapidly to 0, because so little configuration space corresponds to formation of a bond. By referring to (31), we see that for low-temperature ice, n_{HB} should equal 2 when u exceeds -5.3 kcal/mole.

Since the energy of sublimation of ice at its melting point is 11.65 kcal/mole, and the heat of melting is 1.44 kcal/mole,[32] the molar energy of 4°C water compared to separated molecules will be close to 10.2 kcal/mole. Since, furthermore, the coordination number upon melting remains about 4, there is no way of accounting for this energy unless more than three neighbors of any molecule, on the average, participate in hydrogen bonds of no less than 4-kcal/mole energy each. However, the $u = -5$ kcal/mole entry in Table 2 is only 0.5, instead of roughly 1.5, as it should be. Once again we see that approximation (55) produces too little angular correlation between neighbors.

Evidently the local networks of hydrogen bonds that form in liquid water provide extra orientational correlation between nearest neighbors. It is easy to imagine that two such neighbors are embedded in a framework of other water molecules and that this framework acts like a machinist's jig to align the molecules in the correct orientation for hydrogen-bond formation. The implication is that a proper pair-correlation-function theory would specify the $w_\alpha(r_{12})$ in (54) to encompass this "jig effect," and the resultant $g^{(2)}(\mathbf{x}_1, \mathbf{x}_2)$ would yield more realistic g_K and n_{HB} predictions.

Finally we mention that if (53), the Percus–Yevick equation, is integrated over Euler angles for molecules 1 and 2 (while r_{12} is held fixed), and then trial form (55) inserted for $g^{(2)}$, the result constitutes an integral equation for $y(r_{12})$. We have spent considerable effort (though with some simplication of the angular integrations) attempting to solve that integral equation, to compare the result with the "experimental" y in Figure 15. That effort was entirely unsuccessful; no stable solution was found. In retrospect, it seems likely that this failure is symptomatic of the inability of the trial $g^{(2)}$ form in (55) to represent the cooperative aspects of hydrogen-bond network formation in liquid water.

6 Conclusions

Having thus surveyed the applicability of modern techniques in statistical mechanics to liquid water, we now attempt to identify the most likely course of significant progress in the near future.

The specific potential function, $v(\mathbf{x}_1, \mathbf{x}_2)$ in (27), was introduced largely for illustrative purposes. Although we believe it exhibits the major features of the correct water potential, some quantitative revisions will surely be warranted as further information comes to light. Direct quantum-mechanical calcula-

tions of the water pair potential could be of especial value in this regard; but because even a full hydrogen bond represents but a small fraction of the total energy involved in such calculations, this type of investigation must be implemented with great care and precision.

Morokuma and Pedersen[33] have recently carried out a quantum-mechanical computation of the interaction energy of two water molecules in a few selected configurations. They employed molecular orbital theory with a Gaussian basis set of modest proportions. Since their results predict a minimum value of $v(\mathbf{x}_1, \mathbf{x}_2)$ below -12.6 kcal/mole (roughly twice the accepted energy of the hydrogen bond, and certainly much larger than allowed by the measured second virial coefficient), it is certain that more extensive calculations are required. Still, the Morokuma–Pedersen work sets a valuable precedent that should be followed up in the near future.

One aspect of the quantum-mechanical calculations of particular interest would be the tracing out of the angular variation of $v(\mathbf{x}_1, \mathbf{x}_2)$ that is shown in Figure 11 for our own approximate potential. The potential barrier shown in Figure 11 between the SE and SS configurations is clearly a result of idealizing the lone pairs of unshared electrons by point charges, whereas in reality they are rather smeared out spatially. Morokuma and Pedersen[33] calculate that, rather than a barrier, a very shallow minimum should lie between SE and SS; so in fact the most stable configuration for two water molecules would not lie near SE, but near the "interstitial" configuration, I_1, instead. At present it is impossible to tell if this particular aspect of the Morokuma–Pedersen work is an artifact. More accurate molecular orbital calculations could help resolve the issue, although additionally it should be asked if electron correlation might tend to localize the unshared pairs along the characteristic tetrahedral directions. Future quantum-mechanical investigations should not overlook the nuclear distortion of the water molecules as they move relative to one another. This effect conceivably could vary with angle in a way that produces significant effects on the shape of potential curves such as the one in Figure 11. If it should turn out ultimately that the barrier shown in Figure 11 is either too high or altogether absent, the potential (27) could accordingly be modified by use of *three* negative charges, two in the same position as indicated in Figure 3 and one along their bisector (direction $-\mathbf{b}$). Of course the molecule must remain electrically neutral, so with two shielded protons having charges $+\eta e$, the total charge of the three negatives would be $-2\eta e$, as before.

Under the plausible assumption that our quantitative knowledge of $v(\mathbf{x}_1, \mathbf{x}_2)$ will continue to improve, it is important to prognosticate the significant uses of this function. In view of the pessimistic estimates for the direct solution of $g^{(2)}$ integral equations in the near future, an attractive alternative is the Monte Carlo simulation of the thermal behavior of a sample of the molecular fluid.[34,35] In this procedure, an electronic computer moves

a set of several hundred molecules about inside a "vessel," according to Markov chain transition probabilities that are selected to realize a canonical distribution for the temperature of interest (these transition probabilities perforce depend on potential, v). With the presumption of ergodicity, the random motion of these molecules eventually allows any thermodynamic or structural feature of interest to be calculated as an average over the Markovian sequence of system states.

In principle, the full water pair-correlation function $g^{(2)}(\mathbf{x}_1, \mathbf{x}_2)$ could be evaluated by the Monte Carlo technique; but as mentioned earlier, the large number of configurational variables involved makes this impractical. Instead, $\bar{g}^{(2)}(r_{12})$ could be obtained for comparison with experiment, plus a more detailed analysis of the angular correlation of just nearest neighbors to establish the extent of hydrogen-bond bending in the liquid. The importance of hydrogen-bond bending in liquid water has been stressed by Pople.[36]

Since the Monte Carlo method actually produces "typical" liquid-water molecular arrangements, the strongest benefit to be derived from this method would be the pictures that could be made of a small portion of the liquid. Output from an electronic computer can nowadays routinely be used to produce stereoscopic images, and the student interested in water would have the opportunity literally to see how water molecules arrange themselves. The computer could be programmed not only to make the molecules clearly visible but also to indicate where the hydrogen bonds have formed (with suitable choice for B). A result of this submicroscopic view would be a deeper appreciation of the statistics of random hydrogen-bond networks according to probability of formation of polygons of different sizes (squares, pentagons, hexagons, etc.), and according to concentration of various types of faults in the random network (interstitial molecules, free ends, Bjerrum faults, etc.).

The Monte Carlo technique furthermore could be adapted to study of aqueous solutions. A fixed "impurity" can be placed inside the vessel which interacts suitably with the water molecules. For instance, if methane were the solute of interest, a central potential of the Lennard-Jones type would not be inappropriate. One could then study the change in extent and geometrical character of hydrogen bonding around this solute molecule and proceed to assess the current ideas about hydrophobic bonding.[37,38]

Although the Monte Carlo simulation of real water will very likely play an important role in future developments, it certainly must not be considered as an utterly definitive and complete source of knowledge. It is, after all, only a refined (and highly magnified!) sort of experiment on water, and for the most part will only tell us "what," not "why." The Monte Carlo results will eventually require explanations based on analytical theory, in the same way that the integral equation formalism for $g^{(2)}$ nowadays affords explanations for simple fluids (like argon).

There are two reasonable possibilities for "analytical" advances.

1. It is quite conceivable that trial $g^{(2)}$ form (55) could be generalized to represent better the cooperative nature of hydrogen bonding. One possibility would be

$$g^{(2)}(\mathbf{x}_1, \mathbf{x}_2) \simeq y(r_{12}) \exp\left[-\beta z(r_{12}) v(\mathbf{x}_1, \mathbf{x}_2)\right] \tag{61}$$

involving now *two* dimensionless functions just of scalar distance r_{12}. The Percus–Yevick equation (or an alternative integral equation) could then be transformed into a pair of coupled integral equations for the functions y and z, and, one hopes, solved numerically. It is worth noting that, unlike (55), more general expression (61) is consistent with the large-r_{12} limiting pair-correlation behavior determined by (49). In addition, the requirement inferred in the previous section that neighboring particles require more orientational correlation than (55) provides can be accommodated by z exceeding unity at those distances.

2. Bernal's[39,40] admirable intuitive ideas about the coordination geometry of simple liquids deserve an incisive adaptation and application to liquid water. Unlike the simple liquids of spherical molecules, water has the advantage (at least at low temperature) of having definite coordination number 4. The object of a Bernal-type analysis therefore would primarily consist in description of the various types of polyhedra that occur surrounding voids and the statistics of fitting together these polyhedra to form a space-filling network.

Of course it is always risky to predict the future. There is a large chance that our projection for theoretical liquid-water research will prove somewhat misdirected. Nevertheless, significant progress will not come easily in this complicated field, so there is wisdom in attempting to plan effort intelligently. We hope that the present survey will aid scholars of the subject in that important endeavor.

Acknowledgments

The authors are indebted to Dr. J. Rasaiah for suggestions concerning the most effective numerical procedure for evaluating multidimensional integrals encountered in this investigation. We are also grateful to Mr. R. L. Kornegay and Mrs. Z. Wasserman for assistance in the computational aspects of the work.

REFERENCES

1. W. C. Röntgen, *Ann. Phys. Chim.* (*Wied.*), **45**, 91 (1892).
2. H. M. Chadwell, *Chem. Rev.*, **4**, 375 (1927).
3. J. D. Bernal and R. H. Fowler, *J. Chem. Phys.*, **1**, 515 (1933).
4. A convenient survey is provided by J. L. Kavanau, *Water and Solute-Water Interactions*, Holden-Day, San Francisco, 1964.
5. S. A. Rice and P. Gray, *The Statistical Mechanics of Simple Liquids*, Interscience, New York, 1965, Chapter 2.
6. N. Bjerrum, *Kgl. Danske Videnskab. Selskab, Mat.-Fys. Medd.*, **27**, 1 (1951).
7. L. Pauling, *The Nature of the Chemical Bond*, 3rd ed., Cornell University Press, Ithaca, N.Y., 1960, p. 466.
8. H. S. Green, *Proc. Roy. Soc.* (*London*), *Ser. A*, **189**, 103 (1947).
9. F. H. Stillinger, Jr., *Phys. Fluids*, **3**, 725 (1960).
10. J. G. Kirkwood, *J. Chem. Phys.*, **7**, 911 (1939).
11. H. Friedmann, *Physica*, **30**, 921 (1964).
12. W. H. Stockmayer, *J. Chem. Phys.*, **9**, 398 (1941).
13. J. S. Rowlinson, *Trans. Faraday Soc.*, **45**, 974 (1949).
14. J. S. Rowlinson, *J. Chem. Phys.*, **19**, 827 (1951).
15. L. Onsager, *J. Amer. Chem. Soc.*, **43**, 189 (1939).
16. G. A. Jeffrey and R. K. McMullan, *Progr. Inorg. Chem.*, **8**, 43 (1967).
17. J. Corner, *Trans. Faraday Soc.*, **44**, 914 (1948).
18. Ref. 7, Chapter 12.
19. Ref. 7, pp. 467–468.
20. F. Jona and P. Scherrer, *Helv. Phys. Acta*, **25**, 35 (1952).
21. Ref. 7, p. 473.
22. H. S. Frank and A. S. Quist, *J. Chem. Phys.*, **34**, 604 (1961).
23. O. Y. Samoilov, *Structure of Aqueous Electrolyte Solutions*, transl. D. J. G. Ives, Consultants Bureau, New York, 1965.
24. J. E. Mayer and M. G. Mayer, *Statistical Mechanics*, Wiley, 1940, Chapter 16.
25. C. B. Haselgrove, *Math. Comput.*, **15**, 323 (1961).
26. H. Conroy, *J. Chem. Phys.*, **47**, 5307 (1967).
27. G. S. Kell, G. E. McLaurin, and E. Whalley, *J. Chem. Phys.*, **48**, 3805 (1968).
28. J. K. Percus and G. J. Yevick, *Phys. Rev.*, **110**, 1 (1958).
29. A. A. Khan, *Phys. Rev.*, **134**, A367 (1964).
30. A. H. Narten, M. D. Danford, and H. A. Levy, *Discussions Faraday Soc.*, **43**, 97 (1967); see also, A. H. Narten, M. D. Danford, and H. A. Levy, Oak Ridge Natl. Lab. Rept. ORNL-3997, "X-Ray Diffraction Data on Liquid Water in the Temperature Range 4°C–200°C," September 1966.
31. F. E. Harris, E. W. Haycock, and B. J. Alder, *J. Chem. Phys.*, **21**, 1943 (1953).
32. G. Némethy and H. A. Scheraga, *J. Chem. Phys.*, **41**, 680 (1964).
33. K. Morokuma and L. Pedersen, *J. Chem. Phys.*, **48**, 3275 (1968).
34. N. Metropolis, A. W. Rosenbluth, M. N. Rosenbluth, A. H. Teller, and E. Teller, *J. Chem. Phys.*, **21**, 1087 (1953).
35. W. W. Wood, *J. Chem. Phys.*, **48**, 415 (1968).
36. J. A. Pople, *Proc. Roy. Soc.* (*London*), *Ser. A*, **205**, 163 (1951).
37. W. Kauzmann, *Advan. Protein Chem.*, **14**, 1 (1959).
38. G. Némethy, *Angew. Chem.*, **6**, 195 (1967).
39. J. D. Bernal, *Proc. Roy. Inst. G. Brit.*, **37**, 355 (1959).
40. J. D. Bernal, *Sci. Amer.*, **203** (August, 1960), p. 124.